Loading rate dependency of strain energy release rate in mode I delamination of composite laminates

Ekhtiyari, Amin; Alderliesten, René; Shokrieh, Mahmood M.

DOI
10.1016/j.tafmec.2021.102894

Publication date
2021

Document Version
Final published version

Published in
Theoretical and Applied Fracture Mechanics

Theoretical and Applied Fracture Mechanics 112 (2021) 102894

Contents lists available at ScienceDirect

Theoretical and Applied Fracture Mechanics

journal homepage: www.elsevier.com/locate/tafmec

Loading rate dependency of strain energy release rate in mode I delamination of composite laminates

Amin Ekhtiyari [a], René Alderliesten [b], Mahmood M. Shokrieh [a,*]

[a] Composites Research Laboratory, Center of Excellence in Experimental Solid Mechanics and Dynamics, School of Mechanical Engineering, Iran University of Science and Technology, Tehran 16846-13114, Iran

[b] Structural Integrity & Composites Group, Faculty of Aerospace Engineering, Delft University of Technology, Kluyverweg 1, 2629 HS Delft, the Netherlands

ARTICLE INFO

Keywords:
Mode I Delamination
Rate effect
Strain Energy Release Rate
Fracture toughness
CFRP

ABSTRACT

This work aims at studying the loading rate dependency of mode I delamination growth in CFRPs, using typical fracture toughness analysis through both the R-curve and the crack tip opening rate. The average SERR is a method of data reduction based on energy balance which has been previously introduced to characterize delamination growth under different types of loading conditions in a similar manner. In the present research, the application of this method was extended to further analyze the results of delamination experiments at different loading rates. Mode I delamination tests on double cantilever beam specimens were performed at displacement rates varying from standard quasi-static testing up to 400 mm/s. A clear decrease in the propagation fracture toughness as well as in the average SERR was observed at high loading rates. The reduced fracture resistance at elevated rates was physically explained in correlation with fiber bridging, fiber breakage, and matrix cleavage observed in fracture surfaces via scanning electron microscopy.

1. Introduction

Carbon fiber reinforced plastics (CFRPs) are widely used in aerospace structures where high specific strength and stiffness are of great importance. However, due to their relatively poor interlaminar fracture properties, they are vulnerable to delamination. This critical mode of failure results in a noteworthy decrease in stiffness and strength of the laminate and may consequently lead to catastrophic failure of the whole structure. Hence, the examination of different parameters that may affect the delamination growth behavior of composite laminates is necessary toward more damage tolerant designs. Since aeronautical composite structures are intended to carry a variety of realistic loadings, substantial studies have been conducted to characterize the delamination behavior of CFRPs under different loading scenarios including quasi-static [1–4]; fatigue [5–8]; and impact loadings [9–11].

In general, the delamination growth assessment under different quasi-static, dynamic, and fatigue loading conditions has been performed via different methods [12]. However, an appropriate similitude approach to present the experimental data and evaluate the delamination resistance under various loading conditions seems to be necessary to achieve a full understanding of the problem [13]. To this aim, a physics-based method in correlation with the mechanisms involved during the delamination progress has been previously proposed [12,14]. In this method, quasi-static and fatigue delaminations are treated in a similar procedure based on an average strain energy release rate (SERR). In this manner, delamination under quasi-static and fatigue loading are correlated through physical principles. A question arises here that how capable the average SERR method is to be used in studying delamination at monotonic loadings with rates higher than standard quasi-static testing. Different loading cases can cause a wide range of crack tip displacement rates. Remarking that polymeric materials have shown potentially rate-dependent mechanical properties, the loading rate sensitivity of delamination was examined in several researches over the years [15]. Therefore, the application of the average SERR in the field of loading rate dependency analysis is an idea being followed in the present paper.

It is worth mentioning that there are discrepancies among the results found in the literature for the loading rate effects on the delamination growth behavior of CFRPs. In a few papers, increased fracture toughness at loading rates higher than the quasi-static range was reported for the delamination growth of carbon/epoxy composites [16–18]. For instance, a 28% increase in the strain energy release rate with crack velocity was observed in DCB tests of carbon/epoxy samples within a modest range of crosshead speeds up to 8.5 mm/s [16]. Then, the height-

* Corresponding author.
E-mail address: shokrieh@iust.ac.ir (M.M. Shokrieh).

https://doi.org/10.1016/j.tafmec.2021.102894
Received 24 September 2020; Received in revised form 1 January 2021; Accepted 2 January 2021
Available online 7 January 2021

tapered DCB was introduced to achieve higher crack velocities in the same material at test rates up to 460 mm/s [17]. The strain energy release rate increased with crack velocities up to 1 m/s and then dropped slightly. For other brittle carbon/epoxy composites, a 73% increase in fracture toughness was recorded by increasing test speed from 2 mm/s to 120 mm/s [18]. No clear explanation for the ascending trend of the fracture toughness versus the test rate was provided in the above references.

On the contrary, a descending trend in interlaminar fracture resistance with increasing loading rate was found by some other researchers for carbon fiber-reinforced epoxies [19–21] and thermoplastics [19,22–26]. Smiley et al. [19] utilized DCB tests to characterize mode I delamination over a wide range of loading rates up to 670 mm/s. A sudden decrease in SERR calculated by the compliance method was observed due to the change in fracture behavior at elevated test rates. Using a servo-hydraulic test machine to reach crosshead speeds up to 0.19 m/s, Zabala et al. [20] observed a decrease in fracture toughness calculated by the modified beam theory with increasing loading rate for both unidirectional and woven carbon/epoxy composites. While fiber bridging was avoided in their study, the observed descending trend was attributed to less fiber/matrix interface failure and larger matrix brittle cracking. A modified wedge-insert configuration was developed by Thorsson et al. [21] for the measurement of mode I fracture toughness at elevated loading rates. Delamination tests were performed at loading rates ranging from 0.01 mm/s to 3600 mm/s. A correction factor was introduced to the modified beam theory method for measuring the mode I interlaminar fracture toughness using the modified test setup. The reduction in fracture toughness at elevated rate tests was ascribed to the reduced length of the bridging and the process zone.

On the other hand, the loading rate dependency of delamination behavior in carbon/epoxy composites was not significant in the experimental results reported by some other authors [23,25,27,28]. Blackman et al. [25] discussed some aspects of high rate mode I delamination including load introduction and force measurement. In the case of carbon/epoxy laminates, they reported that the value of the fracture toughness remained insensitive to speed through the entire range up to 15 m/s. They derived expressions for the fracture toughness calculation without need for load recording. In [27], the DCB specimen was mounted in a drop tower for high speed testing up to 10 m/s. Almost no influence of loading rate on the mode I fracture toughness of un-tufted and tufted carbon/epoxy non-crimp fabric composites was observed within the analyzed loading range. They introduced analytical expressions for the compliance of the specimen as a function of the crack length and the displacement of one DCB arm. The fracture toughness can then be calculated based on the simple beam theory without load measurement. However, it should be noted that the stiffening effects of fiber bridging will be lost without direct measurement of the applied force.

The different trends of rate effects among previous works in the literature can be attributed to the differences in materials, range of studied test rates, test configurations, and data reduction methods [15] along with possible errors in high rate load and displacement measurements [25]. Thus, it seems that further research is still required to evaluate the delamination growth behavior of composite laminates under various loading rates provided by physical explanations for the observed behavior. The rate sensitivity of fiber bridging should be more concerned to this aim. Based on what is expressed above, the rationale behind the present study is to further examine the loading rate dependency of mode I delamination growth in CFRPs employing the method of average SERR as well as fracture toughness calculation which can establish a correlation between interlaminar fractures under different loadings. In this regard, mode I delamination experiments were performed on DCB specimens made of carbon/epoxy composite panels, varying the displacement rates from 1 mm/min up to 400 mm/s. The delamination growth behavior was studied through both typical interlaminar fracture toughness and the average SERR parameter analysis. Fracture surface inspections using scanning electron microscopy (SEM) were performed to explain the observed loading rate dependency of the fracture mechanisms.

2. Methodology

2.1. Material and specimen preparation

The composite laminates were produced by hand-lay-up of 32 unidirectional carbon/epoxy prepreg layers of M30SC/DT120 (high strength and modulus carbon fiber/toughed thermosetting epoxy) achieving a nominal cured thickness of 4.8 mm. A 12.7 μm Teflon film was inserted in the middle plane of the composite laminates to act as initial delamination. The laminates were cured in a vacuum autoclave at a pressure of 6 bars and curing temperature of 120 °C for 90 min. The plate was cut by a diamond saw into 25 mm width beams with 250 mm length. A pair of aluminum blocks, 25 mm width by 20 mm length with 6 mm thickness, was adhesively bonded to the specimen's end for load introduction.

2.2. Experimental procedure

DCB tests were conducted based on ASTM D5528 standard on a 15 kN servo-hydraulic MTS machine equipped with an HBM high-precision 1 kN Load cell. The load cell is connected to the stationary arm of the test machine, as close to the specimen as possible. This measure helps further reduce possible dynamic effects on load measurement [15]. All tests were performed under displacement control conditions varying the applied displacement rate from 1 mm/min for quasi-static up to 400 mm/s for elevated rates. DCB tests were repeated at least four times at each chosen loading rate. High-speed photography was used to record load line displacement and crack length evolution. In this regard, a Photron Fastcam Camera with a 120 mm Nikon lens was utilized at a 2000 Hz recording speed. The camera system was triggered by the control unit of the test machine. To facilitate the synchronization of the data, the load, displacement, and the synchronized image frames were concurrently recorded by the data acquisition unit. The opening displacements measured by image processing were equal to the displacements directly acquired by the test machine as expected for the loading rates in the range studied here. Further details of the test method along with all the experimental data of this study can be found in the online dataset accompanying this paper [29]. The test set-up is shown in Fig. 1.

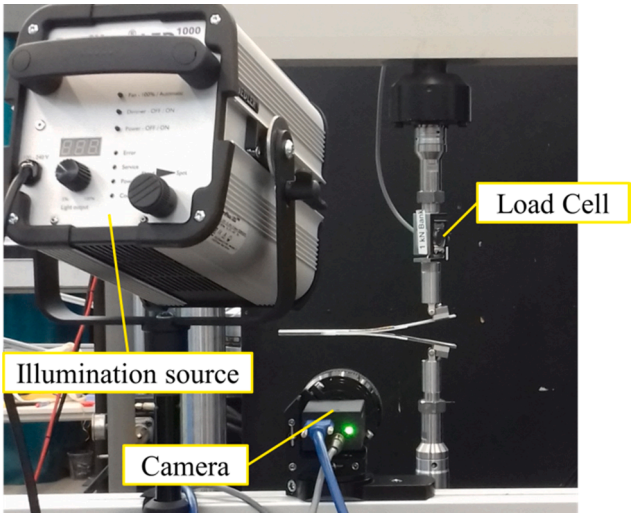

Fig. 1. The DCB test configuration.

2.3. Fracture toughness and the R-curve calculation

Classical data reduction methods developed for quasi-static tests, seem to be capable to provide reliable results for the analysis of DCB tests conducted at intermediate loading rates in the range of the present study as they have been used in similar research works [15]. Three data reduction methods including modified beam theory (MBT), the compliance calibration method (CC), and modified compliance calibration method (MCC) are recommended in ASTM D5528 for characterizing the fracture toughness of DCB specimens. In this study, MBT is chosen as the conservative theory to present the fracture toughness values, although the results of the two other methods differed no more than 5% in comparison. The fracture toughness calculations were done for any increment of at least 1 mm in delamination length to derive the R-curve, noting the fact that generally stable crack propagation was observed in all the analyzed loading rates.

The G_{Ic} is calculated based on MBT as:

$$G_{Ic} = \frac{3P\delta}{2b(a + |\Delta|)} \tag{1}$$

where P and δ are the load and load point displacement respectively. Also, a is the crack length and b represents the width of the beam. Δ is a calibration parameter determined by plotting the cube root of compliance ($C^{1/3}$) versus delamination length (a). The absolute value of the horizontal axis intercept of the $C^{1/3}$-a curve is equal to Δ. The compliance (C) is calculated as the ratio of δ/P.

2.4. Fracture toughness vs. Crack tip opening rate analysis

Some researchers attempted to find a correlation between the measured fracture toughness and a local rate parameter in the vicinity of the crack tip. The crack propagation speed and the crack tip opening displacement rate have attracted more attention in the literature to this aim [15]. The loading rate condition at the crack tip differs from the loading rate of specimen arms and does not remain constant during crack extension. As direct measurement of the opening rate at the crack tip is difficult, Smiley [19] introduced a crack tip opening rate $\dot{y}_{ct}$ at an arbitrary small distance ε from the crack tip. Based on classical beam theory and assuming $\varepsilon \ll a$, $\dot{y}_{ct}$ can be defined as a simple function of the applied loading rate on specimen arms $\dot{\delta}$ and current delamination length a [19]:

$$\dot{y}_{ct} = \frac{3\dot{\delta}\varepsilon^2}{2a^2} \tag{2}$$

The reference distance ε is normally chosen to be two times of the ply thickness that equals 0.3 mm for the specimens tested in the present study. The expression above shows that the crack tip opening rate decreases with increasing delamination length. This approach was applied in the present study to further clarify the rate sensitivity of the fracture toughness as previously done in [21,30].

2.5. The average SERR calculation

The average SERR is obtained only from experimentally measured data rather than using a data reduction scheme based on a theoretical model. In fatigue delamination tests, the load (P), displacement (δ), the crack length (a), and the number of cycles (N) are recorded simultaneously. These data can be presented in a graph plotting da/dN versus dU/dN [31]. For the composite material used in this study, it has been shown that the data points in fatigue loading with different stress ratios align linearly in this graph [31]. For this kind of material as neither plasticity nor other relevant mechanisms cause significant energy dissipation rather than crack extension, the best linear fit to these data must go through the origin. The inverse of the slope of this line corresponds to the average SERR (G^*) based on Eq. (3) [12]:

$$G^* = \frac{1}{b}\frac{dU/dN}{da/dN} = \frac{dU}{dA} \tag{3}$$

in which b is the specimen width. This equation represents the general energy balance introduced by Griffith [32] which is not dependent on the loading condition. It should be noted that the basic assumption in the G^* analysis is that when data in da/dN versus dU/dN graph align along a line, it means that the amount of energy released due to a unit increment in crack length remains unchanged during the crack growth. In other words, the same amount of energy dissipation corresponds to the same amount of crack extension. Thus G^* is defined as a single value for the average release in the strain energy per crack increment under the same loading condition.

To calculate G^* in monotonic loadings (quasi-static and high rate) using the same procedure introduced for fatigue loading, monotonic data points are treated as low-cycle fatigue data. The number of steps or intervals between every two measured data points in monotonic loadings is correlated to the equal number of cycles in fatigue loadings. For example, the interval between two adjacent measured data points can be considered as a single cycle or step. Then, the differences in the value of strain energy and delamination length between those two points are attributed to that step, as illustrated in Fig. 2. The shaded area in this figure typically shows the strain energy dU released due to the crack increment da within the time increment dt. It can be assumed that every single cycle equates to a time increment (dt) which enables the authors to represent G^* in terms of energy released per time increment rate (dU/dt) and crack growth speed (da/dt) based on Eq. (4).

$$G^* = \frac{1}{b}\frac{1}{da/dU} = \frac{1}{b}\frac{dU/dt}{da/dt} = \frac{dU}{dA} \tag{4}$$

The calculation of da, dU, and their time derivatives for each dataset according to each performed test was done based on four different discretization procedures as illustrated in Fig. 3. In each procedure, a different number of steps in da is considered for the same crack growth. Each shaded area in Fig. 3 delimited by dashed lines of the same color is considered as dU corresponding to crack extension da shown by an arrow in the same color between the two relevant data points. Analysis of the same dataset using each of the four different discretization ways in Fig. 3 would result in a cloud of points in $da - dU$ graph. The average of

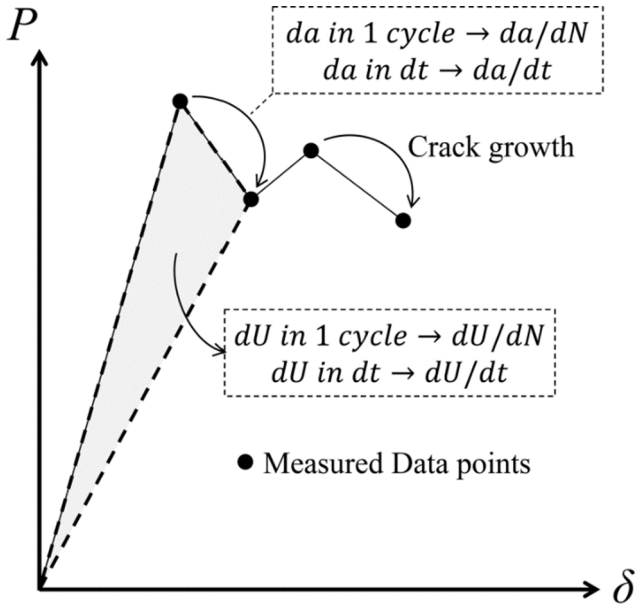

Fig. 2. Schematic load-displacement curve illustrating energy dissipation rate and crack growth speed definitions in the correlated SERR approach.

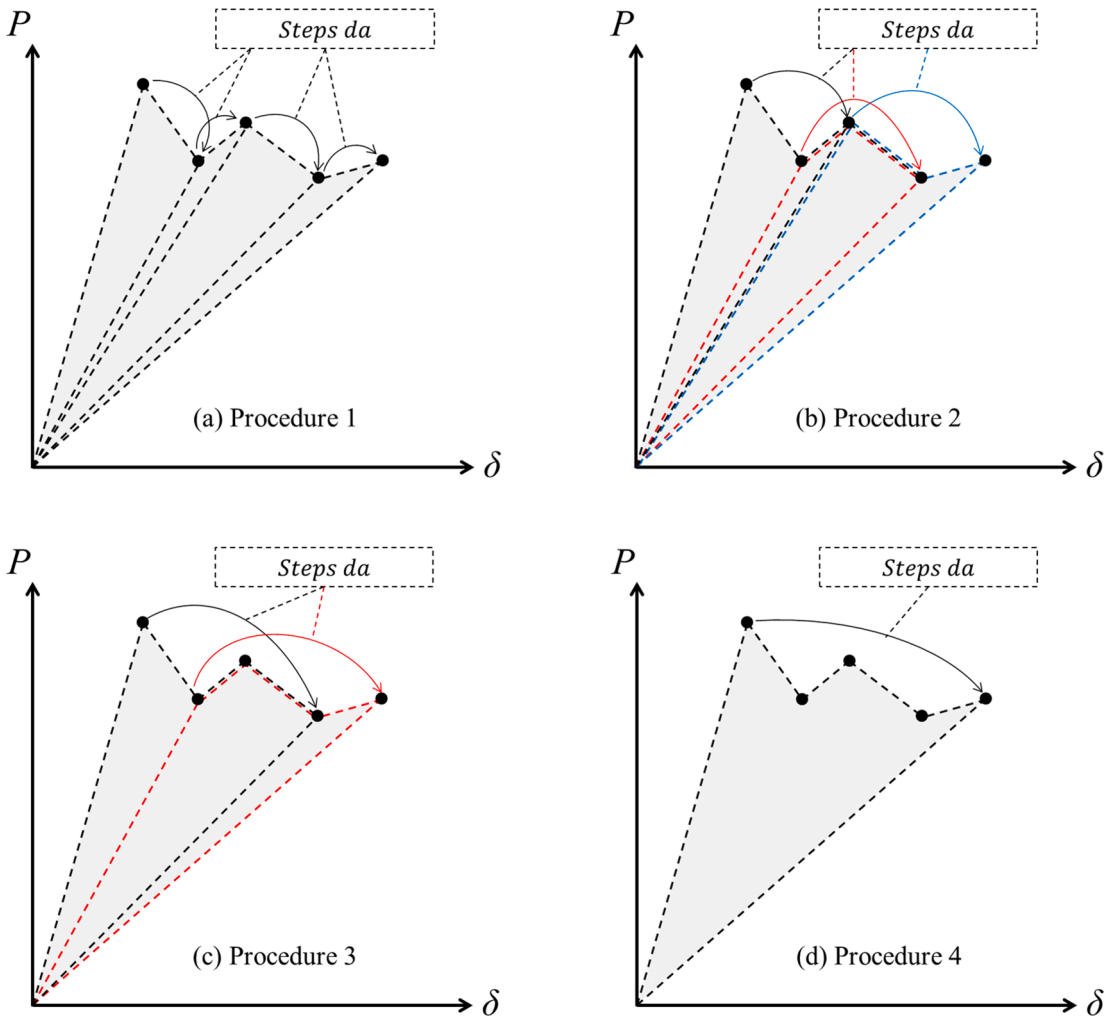

Fig. 3. Schematic discretization of the measured data points to calculate ***dU*** according to steps ***da***.

these points (center of the point cloud) is considered as the desired outcome of the applied discretization procedure on that dataset. Each of the four sets of data at each loading rate was discretized with all the four different ways in Fig. 3, resulting in a group of 16 average points that can be plotted together in one $da - dU$ graph for each loading rate. These points collected in one graph can clearly show the linear trend of da with respect to an increasing dU. A linear regression was used to produce the best linear fit to the data. The slope of the linear fit defines the constant ratio da/dU and G^* value can then be calculated based on Eq. (4), as explained before. Further details on the concept and the calculation procedure of the average SERR can be found in [12]. It should be noted that this method like the other area-based methods [19] does not yield an initiation value of the strain energy release rate nor a delamination resistance curve. Therefore, the standard methods are recommended by ASTM D5528 where the objective is to characterize delamination onset or to derive the R-curve. However, the average SERR method provides results consistent with the outcome of the standard methods and with the physical interpretation of the damage features on fracture surfaces.

3. Results and discussion

Applied load and delamination length versus load line displacement curves of five specimens tested at the five different loading rates analyzed in this study are shown in Fig. 4. A sudden drop in force after reaching a peak value indicates the initiation of delamination growth at all loading rates. This initial unstable crack jump can be seen due to the

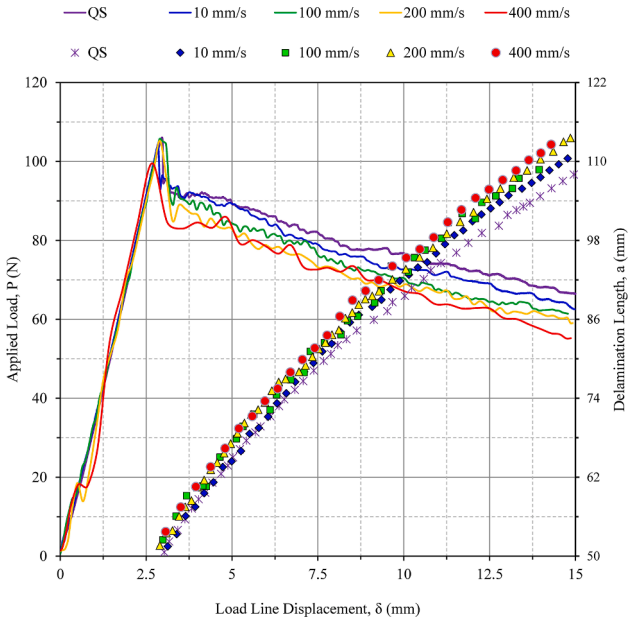

Fig. 4. Load and delamination length versus displacement at the five analyzed loading rates.

effect of a Teflon insert. The peak load variation was within the scatter of the experimental data and thus no significant loading rate effect was detected on the peak load value. However, slightly-longer crack advances after the peak load were observed at elevated loading rates. When crack propagates beyond the initial extension, a consistent descending trend in load vs. displacement curves were observed as crack propagation is intrinsically stable in DCB specimens. In the presence of the fiber bridging, no significant stick–slip behavior occurred during the crack progress in the studied composite material. The stability of growth is not altered by the loading rate as deduced from the curves in Fig. 4. Also, no significant oscillations due to dynamic effects were observed in load curves of high rate tests. However, lower values of force and higher values of the crack extension were measured for a given displacement as the crack propagates at elevated loading rates. The difference in the values of load and crack evolution measured for high rate loadings than for low rate conditions are further pronounced at higher imposed displacements. The more accelerated growth of delamination at high rate tests is the early indication for a reduced fracture resistance compared to the quasi-static case.

Delamination resistance curves (R-curves) of five specimens tested at different loading rates are plotted in Fig. 5. In these curves the variation of G_{Ic} as a function of crack extension is presented for different loading conditions. The initial values of G_{Ic} at different loading rates are approximately the same; although at elevated loading rates a sudden drop in G_{Ic} occurs after the initiation due to the first unstable crack jump from the Teflon insert. The tip of the insert is likely to induce the formation of a resin-rich pocket which blunts the artificial delamination tip and this leads to high values of the fracture toughness at the beginning of the test. The sudden failure of the resin-rich pocket is usually responsible for the above-mentioned unstable crack initiation. Fig. 5 shows that after the initial crack jump, the G_{Ic} value increases with increasing delamination length for all loading rates. When the crack extension exceeds 55 mm in low rate tests and 35–40 mm in elevated rate tests, G_{Ic} remains close to a plateau value ($G_{Ic}^{Prop.}$). This is called the steady state of propagation. The resistance behavior of the composite material indicates the effect of the fiber bridging phenomenon [33]. The number of fibers bridged between adjacent plies behind the crack front increases as the crack propagates. When the bridging process zone in the vicinity of the crack tip is fully developed, the delamination keeps growing in a steady state. The R-curves of different loading conditions in Fig. 5 show a substantial decrease in G_{Ic} for a given delamination length while the loading rate increases. It is clear that by increasing the loading rate, G_{Ic} tends to become plateau earlier at a lower level of delamination length and fracture toughness. It can be concluded that the bridging length and the amount of energy dissipated within the pull-out or breakage of the bridged fibers decrease with increasing loading rate. A similar fiber bridging behavior and loading rate dependency of mode I delamination was previously observed in carbon/epoxy [21] and glass/epoxy composites [30].

In another representation of the typical fracture toughness analysis, Fig. 6 shows the value of G_{Ic} at the steady state of delamination growth (normalized to the quasi-static value of $G_{Ic}^{Prop.}$) as a function of the logarithm of $\dot{y}_{ct}$. These graph provides a better understanding of the loading rate effects on fracture resistance as done in some other similar studies [19,21,30]. It is clear that the fracture toughness linearly decreases with respect to the logarithm of the crack tip opening rate. A descending channel illustrated by two parallel downward lines in Fig. 6 delimits the variation of G_{Ic} vs. $\log\dot{y}_{ct}$ data within the analyzed range of loading rates.

All the results discussed above give clear evidence that the mode I delamination behavior of the composite material being studied here is rate dependent. Now it is intended to explore how this rate effect can be derived from the G^* analysis that was introduced in Section 2.5. All datasets obtained at different loading rates were analyzed by all four different discretization procedures (see Fig. 3) resulting in different point clouds in $da - dU$ graph. For instance, da versus dU analysis of the quasi-static dataset 1 using the discretization procedure 2 is shown in Fig. 7. The resulted cloud of points and the center point are shown by blue and red colors, respectively. The whole set of point clouds for all procedures and all specimens tested are plotted for quasi-static and 400 mm/s loadings in Fig. 8(a) and (b), respectively. Each point in red represents the center of one cloud. The standard deviation from the average values is included within error bars for both da and dU. Fig. 8 shows a generally linear pattern in variation of da against dU. Although a large scatter of data was observed for individual point clouds (see Fig. 7), the overall linear pattern can be revealed when the point clouds or the average points are taken as a whole. A line has been adjusted to the average points and the value of intercept for the best linear fit was achieved very close to zero as expected. The intercept values of the lines shown in Fig. 8(a), (b) are equal to 1.56e-11 and −2.98e-6, respectively. This observation agrees with the fact that crack extension is the only energy dissipating mechanism. The coefficient of determination (R-squared) values presented in Fig. 8(a), (b) verify the quality of fit.

Similar to Fig. 8, linear curves were adjusted to $da - dU$ data for the other three different loading rates applied in this study. The average SERR per steps da denoted by G^* can then be calculated from the slope of the lines by equation (4). The lines with lower slopes would signify crack extensions with more energy consumed per crack area due to more damage features. It was observed that the slope of the linear trend increases with increasing loading rate indicating that less energy is dissipated per area of crack growth at elevated rates. In other words, the energy required for a definite amount of crack growth decreases at high loading rates. This would be equivalent to a descending trend in the variation of G^* as a function of loading rate similar to what was observed

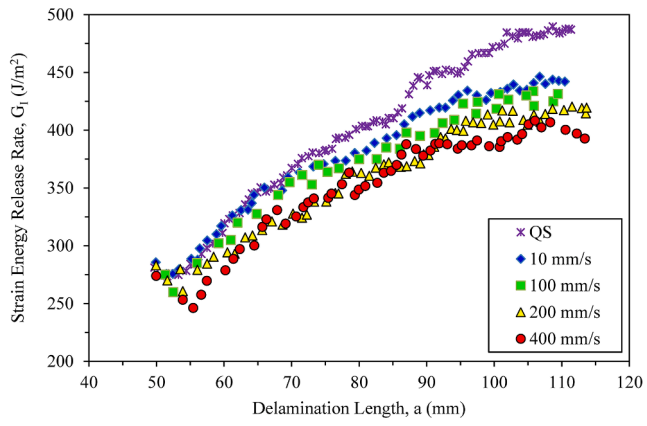

Fig. 5. The R-curve behavior of the DCB specimens under different loading rates.

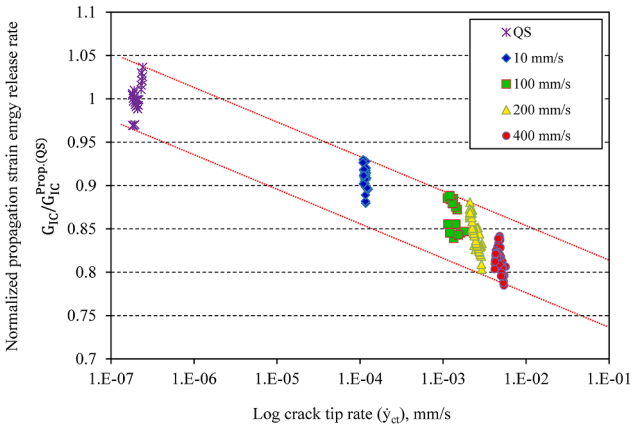

Fig. 6. Normalized fracture toughness versus the logarithm of crack opening displacement rate.

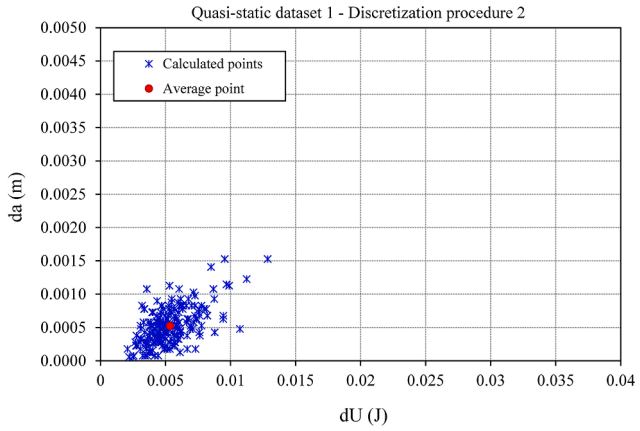

Fig. 7. The outcome of the discretization of quasi-static dataset 1 using procedure 2. The blue markers show the calculated points and the red marker shows the average point. (For interpretation of the references to color in this figure legend, the reader is referred to the web version of this article.)

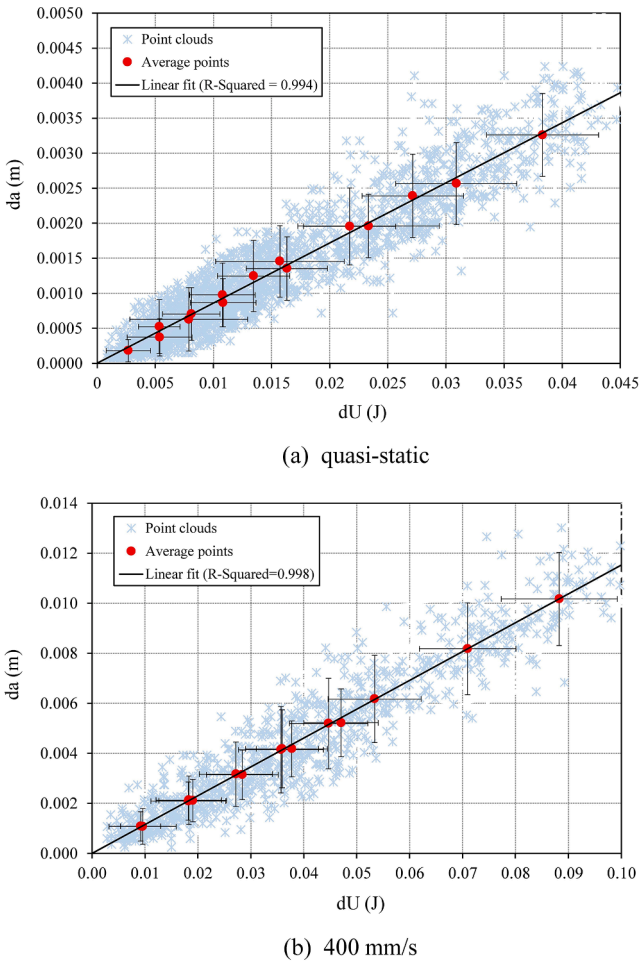

Fig. 8. Linear fit through the average values of ***dU*** and ***da*** for (a) quasi-static and (b) 400 mm/s loading rates.

for the steady-state of fracture toughness G_{Ic}^{Prop} as illustrated in Fig. 9. One should note that G^* is a parameter with a different nature than G_{Ic}. While the latter is calculated through common methods in fracture mechanics, G^* presents a real characteristics based on the physics of delamination growth and not from a theoretical model. In the MBT method for instance, G_{Ic} is derived by the simple cantilever beam model

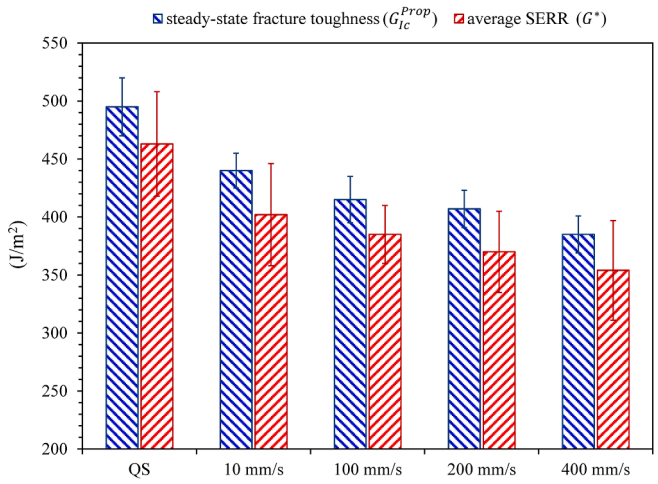

Fig. 9. The steady-state value of the fracture toughness (G_{Ic}^{Prop}) and the average SERR (G^*) at different loading rates.

with a correction factor for the crack-tip rotation and deflection. Distributed loads associated with the fiber bridging behind the crack-tip is not considered in the theory. These limitations of the MBT are manifested in high values for the correction factor and the estimated flexural modulus of the specimen arms. Moreover, within the common methods in fracture mechanics, the energy release rate can be calculated even if there is no crack extension. However, G^* is a parameter that describes the energy released by the crack growth based on the original definition and it is calculated from the measured crack extensions. In fact, the G^* method presents real characteristics in terms of the physics of delamination growth.

The strain energy release rate specifies the amount of damage created per area of crack growth. The more damage mechanisms contribute during delamination, the more energy would be released per crack increments. Different G^* values can signify differences in the damage state and can be reflected in the features of the fracture surfaces. A typical fracture surface of a DCB specimen tested under quasi-static loading captured via scanning electron microscopy (SEM) is shown in Fig. 10. The most common features characteristic of mode I delamination such as fiber bridging, fiber imprints, broken fibers, and areas of cleavage matrix fracture can be seen in this image. Long ligaments of fibers bridged behind the crack front (as shown in Fig. 11) will restrain the crack opening. Then, more energy is dissipated by pull-out, peel-off, and finally breakage of the bridged fibers during crack propagation. The fibers being pulled out of the matrix can induce local shear deformation to the matrix and create shear cusps, although the shear cusps are commonly observed in Mode II delamination [34].

Different levels of fiber bridging due to rate effects can be inferred from the side view pictures shown in Fig. 11. Fracture surfaces of two specimens tested at quasi-static and the maximum applied loading rate are compared in Fig. 12. The SEM image corresponding to the high loading rate presents fewer amounts of either peeled-off or pulled-out fibers. Also, smaller areas of matrix cleavage and fewer shear cusps have led to a smoother fracture surface. This can justify the reduced value of steady-state fracture toughness and G* obtained at increased loading rates.

4. Concluding remarks

Mode I delamination growth in typical DCB specimens made of carbon/epoxy composite laminates has been studied under different loading rates up to 400 mm/s. First, the rate dependency of fracture toughness was testified within classical approaches including both the R-curve and the estimated crack tip opening rate. It was shown that the

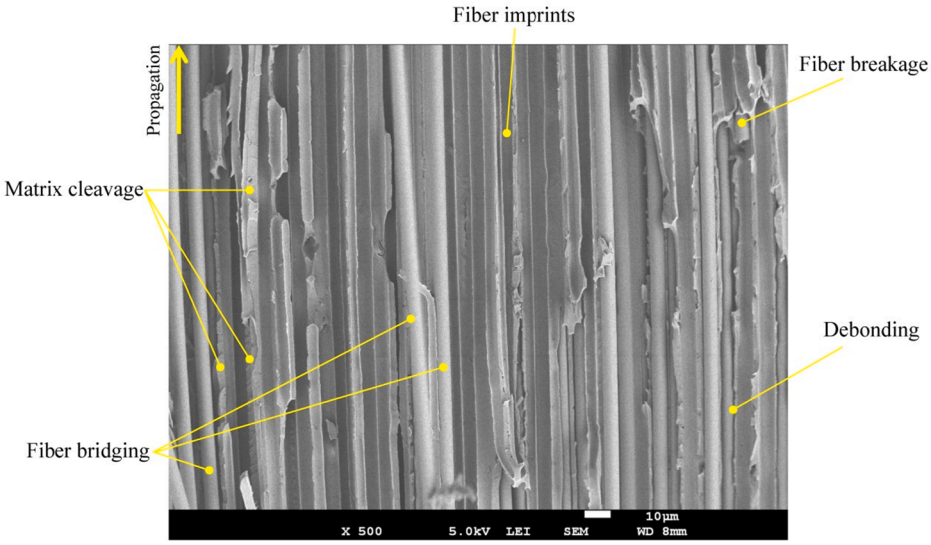

Fig. 10. The fracture surface of mode I delamination at quasi-static loading.

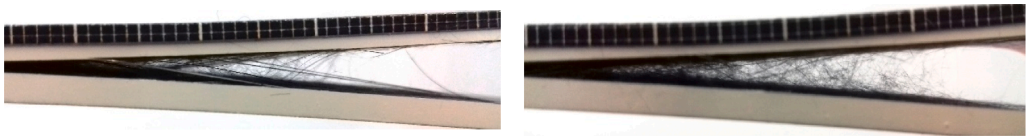

(a) quasi-static loading (b) 400 mm/s loading

Fig. 11. Side view of two tested specimens indicating the lever of fiber bridging.

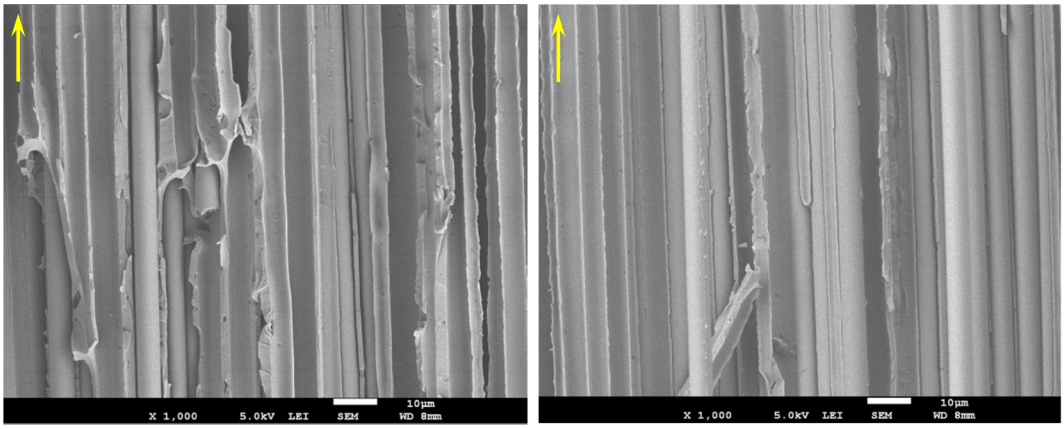

(a) quasi-static loading (b) 400 mm/s loading

Fig. 12. Fracture surfaces at two different loading rates indicate different energy release rate.

fracture toughness decreases with increasing loading rate. A linear descending trend was observed while the fracture toughness at the steady-state of delamination growth was plotted against the logarithm of the local crack tip opening rate. The reduced interlaminar fracture resistance at elevated loading rates was attributed to the decreased contribution of fiber bridging, fiber breakage, and matrix cleavage to energy consumption. Secondly, a new data reduction method utilizing delamination and dissipated energy increments to derive an average SERR was shown to be capable to represent the loading rate effects. By this method, the average SERR named G^* is calculated directly from measured data rather than using a data reduction scheme based on a theoretical model. The method was previously introduced to describe fatigue delamination behavior. Now in this study, it is clearly demonstrated that the method produces results consistent with the outcome of the standard methods even if loading rate effects are concerned. The introduced G^* decreases in monotonic loadings as the crack rate increases. It means that the strain energy released per crack extension decreases at higher propagation speeds. The advantage of the present method is that data from both static and dynamic (elevated rate or fatigue) tests can be studied similarly. To the authors' belief, further research may be conducted to provide a full-scale linkage between the delamination behavior of composite materials under monotonic and fatigue loadings of different rates and frequencies.

CRediT authorship contribution statement

Amin Ekhtiyari: Data curation, Formal analysis, Investigation, Software, Writing - original draft. **René Alderliesten:** Conceptualization, Investigation, Methodology, Project administration, Supervision, Resources, Validation, Writing - review & editing. **Mahmood M. Shokrieh:** Conceptualization, Funding acquisition, Investigation, Methodology, Project administration, Resources, Supervision, Validation, Writing - review & editing.

Declaration of Competing Interest

The authors declare that they have no known competing financial interests or personal relationships that could have appeared to influence the work reported in this paper.

Acknowledgment

This research was supported by Iran National Science Foundation (INSF), Grant No. 97024007.

References

[1] Z. Daneshjoo, L. Amaral, R.C. Alderliesten, M.M. Shokrieh, M. Fakoor, Development of a physics-based theory for mixed mode I/II delamination onset in orthotropic laminates, Theor. Appl. Fract. Mech. 103 (2019), 102303, https://doi.org/10.1016/j.tafmec.2019.102303.

[2] Y. Gong, B. Zhang, L. Zhao, J. Zhang, N. Hu, C. Zhang, R-curve behaviour of the mixed-mode I/II delamination in carbon/epoxy laminates with unidirectional and multidirectional interfaces, Compos. Struct. 223 (2019), 110949, https://doi.org/10.1016/j.compstruct.2019.110949.

[3] Y. Gong, L. Zhao, J. Zhang, Y. Wang, N. Hu, Delamination propagation criterion including the effect of fibre bridging for mixed-mode I/II delamination in CFRP multidirectional laminates, Compos. Sci. Technol. 151 (2017) 302–309, https://doi.org/10.1016/j.compscitech.2017.09.002.

[4] T.A. Sebaey, N. Blanco, J. Costa, C.S. Lopes, Characterization of crack propagation in mode I delamination of multidirectional CFRP laminates, Compos. Sci. Technol. 72 (2012) 1251–1256, https://doi.org/10.1016/j.compscitech.2012.04.011.

[5] R. Jones, A.J. Kinloch, J.G. Michopoulos, A.J. Brunner, N. Phan, Delamination growth in polymer-matrix fibre composites and the use of fracture mechanics data for material characterisation and life prediction, Compos. Struct. 180 (2017) 316–333, https://doi.org/10.1016/j.compstruct.2017.07.097.

[6] L. Yao, H. Cui, Y. Sun, L. Guo, X. Chen, M. Zhao, R.C. Alderliesten, Fibre-bridged fatigue delamination in multidirectional composite laminates, Compos. Part A Appl. Sci. Manuf. 115 (2018) 175–186, https://doi.org/10.1016/j.compositesa.2018.09.027.

[7] L. Amaral, R. Alderliesten, R. Benedictus, Understanding mixed-mode cyclic fatigue delamination growth in unidirectional composites: An experimental approach, Eng. Fract. Mech. 180 (2017) 161–178, https://doi.org/10.1016/j.engfracmech.2017.05.049.

[8] J. Hoffmann, G. Scharr, Mode I delamination fatigue resistance of unidirectional and quasi-isotropic composite laminates reinforced with rectangular z-pins, Compos. Part A Appl. Sci. Manuf. 115 (2018) 228–235, https://doi.org/10.1016/j.compositesa.2018.10.013.

[9] H.R. Wang, S.C. Long, X.Q. Zhang, X.H. Yao, Study on the delamination behavior of thick composite laminates under low-energy impact, Compos. Struct. 184 (2018) 461–473, https://doi.org/10.1016/j.compstruct.2017.09.083.

[10] S. Long, X. Yao, X. Zhang, Delamination prediction in composite laminates under low-velocity impact, Compos. Struct. 132 (2015) 290–298, https://doi.org/10.1016/j.compstruct.2015.05.037.

[11] R.A. Govender, G.S. Langdon, G.N. Nurick, T.J. Cloete, Impact delamination testing of fibre reinforced polymers using Hopkinson Pressure Bars, Eng. Fract. Mech. 101 (2013) 80–90, https://doi.org/10.1016/j.engfracmech.2012.07.025.

[12] L. Amaral, L. Yao, R. Alderliesten, R. Benedictus, The relation between the strain energy release in fatigue and quasi-static crack growth, Eng. Fract. Mech. 145 (2015) 86–97, https://doi.org/10.1016/j.engfracmech.2015.07.018.

[13] J.A. Pascoe, R.C. Alderliesten, R. Benedictus, Methods for the prediction of fatigue delamination growth in composites and adhesive bonds – A critical review, Eng. Fract. Mech. 112–113 (2013) 72–96, https://doi.org/10.1016/j.engfracmech.2013.10.003.

[14] R.C. Alderliesten, How proper similitude can improve our understanding of crack closure and plasticity in fatigue, Int. J. Fatigue. 82 (2016) 263–273, https://doi.org/10.1016/j.ijfatigue.2015.04.011.

[15] M. May, Measuring the rate-dependent mode I fracture toughness of composites - A review, Compos. Part A., Appl. Sci. Manuf. 81 (2016) 1–12, https://doi.org/10.1016/j.compositesa.2015.10.033.

[16] A.A. Aliyu, I.M. Daniel, Effects of strain rate on delamination fracture toughness of graphite/epoxy, Delamination Debonding Mater. ASTM STP 876. (1985) 336–348.

[17] G. Yaniv, I.M. Daniel, Height-tapered double cantilever beam specimen for study of rate effects on fracture toughness of composites, ASTM Spec. Tech. Publ. (1988) 241–258. Doi: 10.1520/STP26139S.

[18] H. You, Y.-J. Yum, Loading Rate Effect on Mode I Interlaminar Fracture of Carbon/Epoxy Composite, J. Reinf. Plast. Compos. 16 (1997) 537–549, https://doi.org/10.1177/073168449701600604.

[19] A.J. Smiley, R.B. Pipes, Rate Effects on Mode I Interlaminar Fracture Toughness in Composite Materials, J. Compos. Mater. 21 (1987) 670–687, https://doi.org/10.1177/002199838702100706.

[20] H. Zabala, L. Aretxabaleta, G. Castillo, J. Aurrekoetxea, Loading rate dependency on mode I interlaminar fracture toughness of unidirectional and woven carbon fibre epoxy composites, Compos. Struct. 121 (2015) 75–82, https://doi.org/10.1016/j.compstruct.2014.11.001.

[21] S.I. Thorsson, A.M. Waas, J. Schaefer, B. Justusson, S. Liguore, Effects of elevated loading rates on mode I fracture of composite laminates using a modified wedge-insert fracture method, Compos. Sci. Technol. 156 (2018) 39–47, https://doi.org/10.1016/j.compscitech.2017.12.018.

[22] S. Mall, G.E. Law, M. Katouzian, Loading Rate Effect on Interlaminar Fracture Toughness of A Thermoplastic Composite, J. Compos. Mater. 21 (1987) 569–579, https://doi.org/10.1177/002199838702100607.

[23] J.W. Gillespie, L.A. Carlsson, A.J. Smiley, Rate-dependent mode I interlaminar crack growth mechanisms in graphite/epoxy and graphite/PEEK, Compos. Sci. Technol. 28 (1987) 1–15, https://doi.org/10.1016/0266-3538(87)90058-3.

[24] R. Fracasso, M. Rink, A. Pavan, R. Frassine, The effects of strain-rate and temperature on the interlaminar fracture toughness of interleaved PEEK/CF composites, Compos. Sci. Technol. 61 (2001) 57–63, https://doi.org/10.1016/S0266-3538(00)00153-6.

[25] B.R.K. Blackman, J.P. Dear, A.J. Kinloch, H. Macgillivray, Y. Wang, J.G. Williams, P. Yayla, The failure of fibre composites and adhesively bonded fibre composites under high rates of test, J. Mater. Sci. 30 (1995) 5885–5900, https://doi.org/10.1007/BF01151502.

[26] P. Beguelin, M. Barbezat, H.H. Kausch, Mechanical characterization of polymers and composites with a servohydraulic high-speed tensile tester, J. Phys. III (1) (1991) 1867–1880, https://doi.org/10.1051/jp3:1991238.

[27] M. Colin de Verdiere, A.A. Skordos, M. May, A.C. Walton, Influence of loading rate on the delamination response of untufted and tufted carbon epoxy non crimp fabric composites: Mode I, Eng. Fract. Mech. 96 (2012) 11–25, https://doi.org/10.1016/j.engfracmech.2012.05.015.

[28] G. Hug, P. Thévenet, J. Fitoussi, D. Baptiste, Effect of the loading rate on mode I interlaminar fracture toughness of laminated composites, Eng. Fract. Mech. 73 (2006) 2456–2462, https://doi.org/10.1016/j.engfracmech.2006.05.019.

[29] A. Ekhtiyari, Loading rate effects on the Mode I delamination growth of laminated carbon/epoxy composite DCB specimens, 4TU, Cent. Res. Data. (2019), https://doi.org/10.4121/uuid:70505d03-0a81-4497-ba73-92a3b4563c2a.

[30] A. Ekhtiyari, M.M. Shokrieh, R. Alderliesten, Loading rate effects on mode-I delamination in glass/epoxy and glass/CNF/epoxy laminated composites, Eng. Fract. Mech. 228 (2020), 106908, https://doi.org/10.1016/j.engfracmech.2020.106908.

[31] L. Yao, R.C. Alderliesten, M. Zhao, R. Benedictus, Discussion on the use of the strain energy release rate for fatigue delamination characterization, Compos. Part A Appl. Sci. Manuf. 66 (2014) 65–72, https://doi.org/10.1016/j.compositesa.2014.06.018.

[32] A.A. Griffith, The phenomena of rupture and flow in solids, Philos. Trans. R. Soc. A Math. Phys. Eng. Sci. 221 (1921) 163–198, https://doi.org/10.1098/rsta.1921.0006.

[33] L. Yao, R. Alderliesten, M. Zhao, R. Benedictus, Bridging effect on mode I fatigue delamination behavior in composite laminates, Compos. Part A Appl. Sci. Manuf. 63 (2014) 103–109, https://doi.org/10.1016/j.compositesa.2014.04.007.

[34] E.S. Greenhalgh, Ed., Delamination-dominated failures in polymer composites, in: Fail. Anal. Fractography Polym. Compos., Elsevier, 2009: pp. 164–237. Doi: 10.1533/9781845696818.164.